

Effect of substrate type on Ni self-assembly process

Xuzhao Chai(柴旭朝), Boyang Qu(瞿博阳), Yuechao Jiao(焦岳超), Ping Liu(刘萍), Yanxia Ma(马彦霞), Fengge Wang(王凤歌), Xiaoquan Li(李晓荃), Xiangqian Fang(方向前), Ping Han(韩平), Rong Zhang(张荣)

Citation: Chin. Phys. B . 2019, 28(1): 016102. **doi:** 10.1088/1674-1056/28/1/016102
Journal homepage: http://cpb.iphy.ac.cn; http://iopscience.iop.org/cpb

What follows is a list of articles you may be interested in

Performance improvement in polymeric thin film transistors using chemically modified both silver bottom contacts and dielectric surfaces

Xie Ying-Tao, Ouyang Shi-Hong, Wang Dong-Ping, Zhu Da-Long, Xu Xin, Tan Te, Fong Hon-Hang
Chin. Phys. B . 2015, 24(9): 096803. **doi:** 10.1088/1674-1056/24/9/096803

Microstructure evolution of Cu atomic islands on liquid surfaces in the ambient atmosphere

Zhang Xiao-Fei, Chen Hang, Yu Sen-Jiang
Chin. Phys. B . 2015, 24(7): 076103. **doi:** 10.1088/1674-1056/24/7/076103

Fabrication of VO_2 thin film by rapid thermal annealing in oxygen atmosphere and its metal-insulator phase transition properties

Liang Ji-Ran, Wu Mai-Jun, Hu Ming, Liu Jian, Zhu Nai-Wei, Xia Xiao-Xu, Chen Hong-Da
Chin. Phys. B . 2014, 23(7): 076801. **doi:** 10.1088/1674-1056/23/7/076801

Scanning tunneling microscopy study of molecular growth structures of $Gd@C_{82}$ on Cu(111)

Chen Jian, Qin Zhi-Hui, Pan Jin-Bo, Lu Shuang-Zan, Du Shi-Xuan, Gao Hong-Jun, Cao Geng-Yu
Chin. Phys. B . 2013, 22(7): 076802. **doi:** 10.1088/1674-1056/22/7/076802

Kinetic Monte Carlo simulations of optimization of self-assembly quantum rings growth strategy based on substrate engineering

Liu Jian-Tao, Feng Hao, Yu Zhong-Yuan, Liu Yu-Min, Shi Qiang, Song Xin, Zhang Wen, Peng Yi-Wei
Chin. Phys. B . 2013, 22(4): 046801. **doi:** 10.1088/1674-1056/22/4/046801

Effect of substrate type on Ni self-assembly process*

Xuzhao Chai(柴旭朝)[1,†], Boyang Qu(瞿博阳)[1,‡], Yuechao Jiao(焦岳超)[1], Ping Liu(刘萍)[1], Yanxia Ma(马彦霞)[1], Fengge Wang(王凤歌)[1], Xiaoquan Li(李晓荃)[1], Xiangqian Fang(方向前)[1], Ping Han(韩平)[2], and Rong Zhang(张荣)[2]

[1] *School of Electric and Information Engineering, Zhongyuan University of Technology, Zhengzhou* 450007, *China*
[2] *School of Electronic Science and Engineering, Nanjing University, Nanjing* 210093, *China*

(Received 13 June 2018; revised manuscript received 12 September 2018; published online 12 December 2018)

Ni self-assembly has been performed on GaN (0001), Si (111) and sapphire (0001) substrates. Scanning electron microscopy (SEM) images verify that the Si (111) substrate leads to failure of the Ni assembly due to Si–N interlayer formation; the GaN (0001) and sapphire (0001) substrates promote assembly of the Ni particles. This indicates that the GaN/sapphire (0001) substrates are fit for Ni self-assembly. For the Ni assembly process on GaN/sapphire (0001) substrates, three differences are observed from the x-ray diffraction (XRD) patterns: (i) Ni self-assembly on the sapphire (0001) needs a 900 °C annealing temperature, lower than that on the GaN (0001) at 1000 °C, and loses the Ni network structure stage; (ii) the Ni particle shape is spherical for the sapphire (0001) substrate, and truncated-cone for the GaN (0001) substrate; and (iii) a Ni–N interlayer forms between the Ni particles and the GaN (0001) substrate, but an interlayer does not appear for the sapphire (0001) substrate. All these differences are attributed to the interaction between the Ni and the GaN/sapphire (0001) substrates. A model is introduced to explain this mechanism.

Keywords: self-assembly, thermal annealing, substrates

PACS: 61.46.–w, 68.08.Bc, 68.35.Fx **DOI:** 10.1088/1674-1056/28/1/016102

1. Introduction

The self-assembly of nanometer-sized metal and semiconductor particles has become of considerable importance, and it is an attractive approach for fabricating intrinsic nano-scale devices without the need for expensive lithography.[1,2] Self-assembly is a bottom-up approach, allowing the fabrication of the regular array structures such as quantum wells, wires and dots. Many methods have been applied to achieve the self-assembly of nanoparticles. For example, pulsed lasers have been used to assemble Au, Ag, Ni, and Ti nanoparticles,[3] and ion sputtering as a method has been applied to form nano-scale GaSb dots.[4] In addition, thermal annealing is also a good method for obtaining self-assembled particles.[5,6] This method has two steps, as follows: the first step is the metal deposition on the substrate surface; the second step is the thermal annealing treatment of the metal films.

The self-assembly technique assisted by thermal annealing is easily controlled, and is widely applied to fabricate nanostructures. Many reports have revealed that the metal films have been assembled into metal nanoparticles by thermal annealing.[7–9] Chhowalla *et al.* have applied self-assembled particles to induce the growth of vertically aligned carbon nanotubes, and have directly controlled the nanotube diameter, growth rate and density by adjusting the self-assembled particle size.[10] The self-assembled Ni particles have acted as nano-masks to fabricate GaN nano-rods for enhancing light output power efficiency.[11] The assistance of self-assembly simplifies the nano-rod fabrication, and even drives the achievement of fabrication of InGaN/GaN nano-rod light-emitting diodes (LEDs).[1,2] According to these reports, the self-assembly process has a great effect on nanostructure fabrication, and the formation of the self-assembled particles depends strongly on the thermal annealing treatment. Therefore, the optimization of the annealing parameters is crucial for the self-assembly process, including annealing temperature and annealing time.

Many reports have confirmed that the self-assembled particle size depends on the thermal annealing stage and the metal-film thickness. High annealing temperature, ranging from 600 °C to 1000 °C, has driven Fe, Cu and Pd films to assemble nano-dots.[7] Low annealing temperatures (300–500 °C) also meet the temperature requirement for assembled particles, but the annealing time can reach up to 30 min.[8] Moreover, metal-film thickness plays a key role in the size and shape of the self-assembled particle.[9] All these reports mainly refer to the application, density and size of the self-assembled particles, and little attention has been given to the effect of the substrates on the self-assembly process.

*Project supported by the National Natural Science Foundation of China (Grant Nos. 61473266 and 61673404), the Program for Science&Technology Innovation Talents in Universities of Henan Province, China (Grant No. 16HASTIT033), the Science and Technique Foundation of Henan Province, China (Grant Nos. 132102210521, 152102210153, 182102210516, and 172102210601), the Key Program in Universities of Henan Province, China (Grant No. 17B520044), and the Science and Technique Project of the China National Textile and Apparel Council (Grant No. 2018104).

†Corresponding author. E-mail: xzchai@zut.edu.cn
‡Corresponding author. E-mail: 6509@zut.edu.cn

© 2019 Chinese Physical Society and IOP Publishing Ltd

In this work, we study Ni self-assembly on sapphire (0001), GaN (0001) and Si (111) substrates. The effect of these substrates on the self-assembled Ni particles is discussed. The evolution of the self-assembled particle morphology with annealing time is shown, and the corresponding mechanism is also analyzed.

2. Experiments

Sapphire (0001), GaN (0001) and Si (111) substrates were cut into pieces of around 1 cm×1 cm in size. Here, 3 μm thick GaN films deposited on sapphire (0001) served as the GaN (0001) substrates; the sapphire (0001) and Si (111) substrates were directly selected from commercial wafers. These pieces were cleaned using a standard three-stage ultrasonic solvent clean (acetone, methanol and isopropanol) and deionized water. Prior to deposition, the substrates were subjected to a glow discharge under high vacuum to improve the adhesion of the Ni films to the substrates. Ni films with a thickness of 10 nm were simultaneously sputtered on these three substrates with the base pressure of $\sim 1 \times 10^{-6}$ Torr. Thicknesses were determined by a quartz crystal oscillator with an accuracy of ±0.1 nm during the deposition. Finally, all the Ni pieces were annealed at a series of different temperatures to achieve the Ni self-assembly process. The corresponding annealing time and ambient were 3 min and N_2, respectively.

The self-assembled Ni particles were characterized using x-ray diffraction (XRD) and scanning electron microscopy (SEM). XRD measurements were carried out using the Philips X' Pert Pro x-ray diffractometer with Cu $K\alpha$ line for the identification of crystallographic phases and their grain size. SEM and cross-sectional SEM experiments were also employed to study the morphology of the Ni particles.

3. Results and discussion

Figure 1 shows the morphology of the Ni films on the GaN (0001) substrates after the thermal annealing treatment. Some pin-pits are exhibited on the surface at the annealing temperature of 700 °C, compared with the as-grown sample (as shown by the red arrows in Fig. 1(b)). The pin-pit size gradually increases with annealing temperature, and these pin-pits merge into a network structure at 850 °C (Figs. 1(c) and 1(d)). As the annealing temperature gradually rises, the network morphology evolves into a ribbon structure, and eventually into sphere-like particles. At 1000 °C, the Ni particles are fully assembled and are distributed randomly on the surface (Fig. 1(h)).

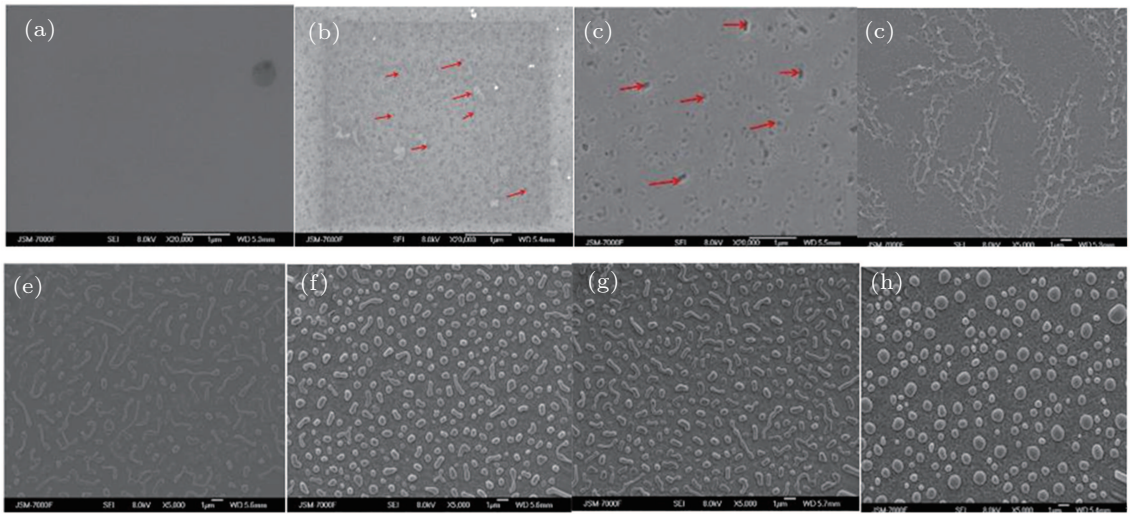


Fig. 1. Top-view SEM images of the Ni films on GaN (0001) substrates after annealing at different temperatures: (a) as-grown, (b) 700 °C, (c) 750 °C, (d) 850 °C, (e) 870 °C, (f) 920 °C, (g) 950 °C, (h) 1000 °C. The red arrows show the pin-pit positions.

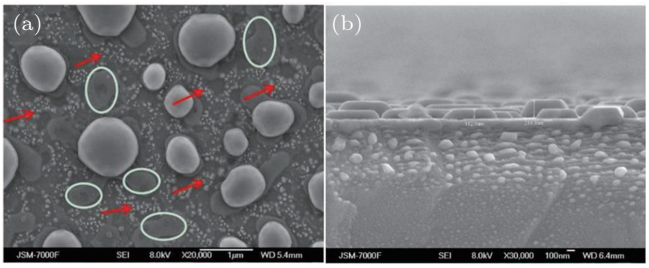


Fig. 2. High resolution SEM images of the Ni particles at the annealing temperature of 1000 °C: (a) top-view, (b) cross-section. The white ovals show the remnants of the ribbon structure, and the red arrows show the Ni nano-dots.

In order to reveal further the morphology of the Ni particles on GaN (0001) substrates, high resolution SEM scanning was carried out for the Ni particles assembled at 1000 °C (Fig. 2). The Ni particles have a truncated-cone shape and their height ranges from 116 nm to 219 nm, which is confirmed by the cross-sectional image (see Fig. 2(b)). These particles display three features in Fig. 2(a): (i) the particle size is not uniform, ranging from 502 nm to 1.1 μm; (ii) irregular terraces are distributed around the particles, and probably originate from the remnants of the ribbon structure (as shown by

the white ovals in Fig. 2(a)); and (iii) small Ni nano-dots are scattered around the Ni particles (as shown by the red arrows in Fig. 2).

The self-assembly process of the Ni films on sapphire (0001) substrate is shown in Fig. 3. Similarly, pin-pits appear on the surface of the sample annealed at 700 °C. The density is much higher, so that one cannot see clearly. This is attributed to the smaller Ni crystalline grain and the higher grain boundary density.[12] The Ni film on the sapphire immediately evolves into a ribbon structure as the annealing temperature increases up to 750 °C. The ribbon structure is similar to that of the Ni films on the GaN (0001) annealed at 870 °C (as shown in Figs. 1(e) and 3(b)). But the annealed Ni films on the sapphire (0001) do not show the network structure stage, and are directly assembled into the spherical particles at 800 °C. The self-assembled Ni particles do not exhibit the same features as those on the GaN (0001) at 1000 °C.

A more detailed statistical analysis of the particle size has been carried out for the self-assembled Ni particles on the sapphire (0001) substrate. Figure 4 gives the histogram analysis of the original SEM images. The resulting histogram is well fitted by a Gaussian distribution. For the sample annealed at 750 °C, the mean diameter and the number of Ni particles are 175 nm and 186, respectively. As the temperature reaches 900 °C, the mean diameter increases up to 250 nm, and the number decreases down to 63 (Fig. 4). Obviously, the temperature increase results in trends of growing mean diameter and decreasing number. In this evolution, the smaller Ni particles gradually shrink, and even diminish; the larger particles increasingly expand (Fig. 3). The evolution is just a mass transport process, which is attributed to the surface diffusion of the Ni atoms.

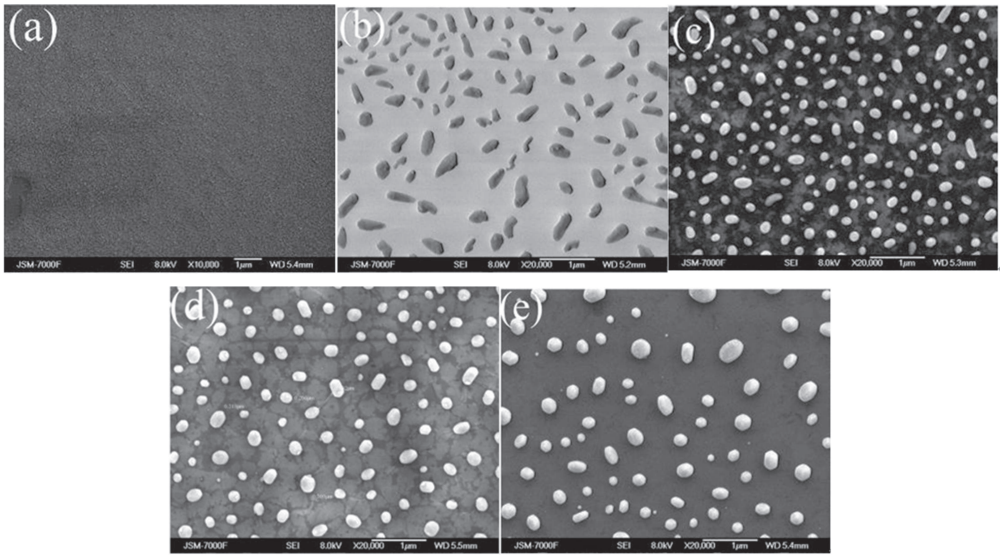


Fig. 3. SEM images of the Ni film on sapphire (0001) after annealing at different temperatures: (a) 700 °C, (b) 750 °C, (c) 800 °C, (d) 850 °C, (e) 900 °C.

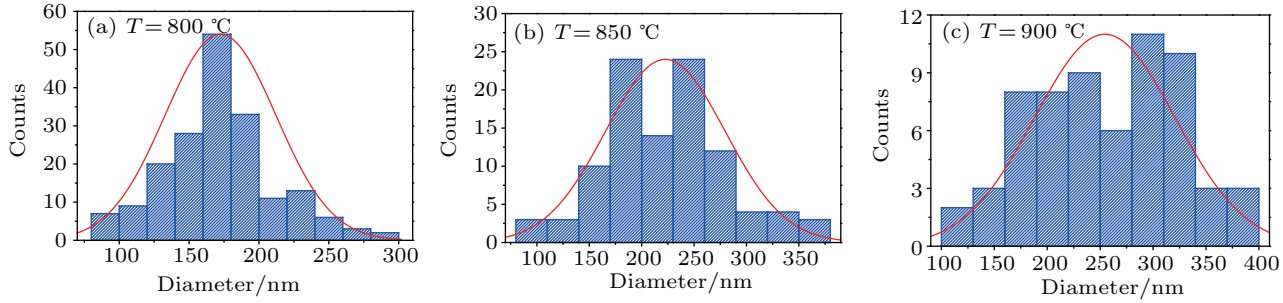


Fig. 4. Particle size distribution histograms obtained by analyzing the SEM images: (a) 800 °C, (b) 850 °C, (c) 900 °C.

Si (111) as the most common substrate is selected for the Ni self-assembly, so that we can further study the substrate effect on the Ni self-assembly process. The annealing of the Ni films on the Si (111) substrates is shown in Fig. 5. The sample annealed at 700 °C features high density pin-pits, and is similar to the Ni films on the GaN/sapphire (0001) substrates. The pin-pits evolve into holes as the temperature reaches 800 °C (Fig. 5(b)). These holes expand and become more apparent at 900 °C (Fig. 5(c)). The holes are generally located at the grain boundaries, separating grains from one another.[13] The Ni films on the Si (111) substrate during the annealing do not show self-assembled particles as those on the sapphire/GaN

(0001) substrates. Therefore, the Si (111) substrate is not a promising candidate for Ni self-assembly as compared with the GaN/sapphire (0001) substrates. Obviously, this mechanism differs from the self-assembly mechanism. During the annealing process, the diffusion of the Ni to the silicon leads to form the Ni–Si interlayer, especially at higher annealing temperature. And even the vacancies left accumulate to form visible holes.[13]

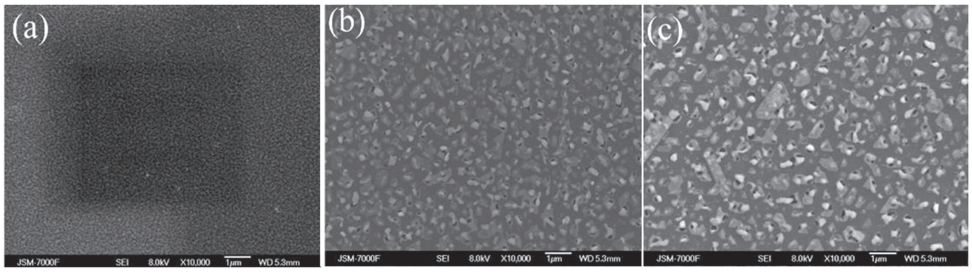


Fig. 5. The Ni film annealing on the Si (111) substrate: (a) 700 °C; (b) 800 °C; (c) 900 °C.

In order to clarify the self-assembly mechanism, XRD measurements were performed for the annealed Ni films on the sapphire/GaN (0001) substrates. Figure 6 shows the XRD spectra of the annealed Ni film on the GaN (0001) substrate. The XRD spectrum of the as-grown sample shows the diffraction peaks from the GaN (0001) substrate, such as GaN (002), 34.5° (2θ) and GaN (004), 72.9° (2θ); the peak at 41.6° is attributed to the sapphire (006). Additionally, the peaks located at 44.6° and 52.9° originate from the (111) and (200) of the fcc Ni, respectively.[14] The features of the XRD spectra do not change for the samples annealed at 870 °C and 920 °C (Figs. 6(b) and 6(c)). However, as the annealing temperature increases to 950 °C, a peak at 46.0° appears around the Ni (111) peak, resulting from the Ni_xN (200).[12] This verifies that a Ni–N interlayer forms due to high-temperature diffusion. At a temperature of 1000 °C, more N atoms diffuse into the Ni lattice structure to replace the Ni atoms. This fact contributes to an apparent increase in the Ni_xN (200) peak intensity (Fig. 6(e)). The corresponding peak position even moves from 46.0° to 44.7°.

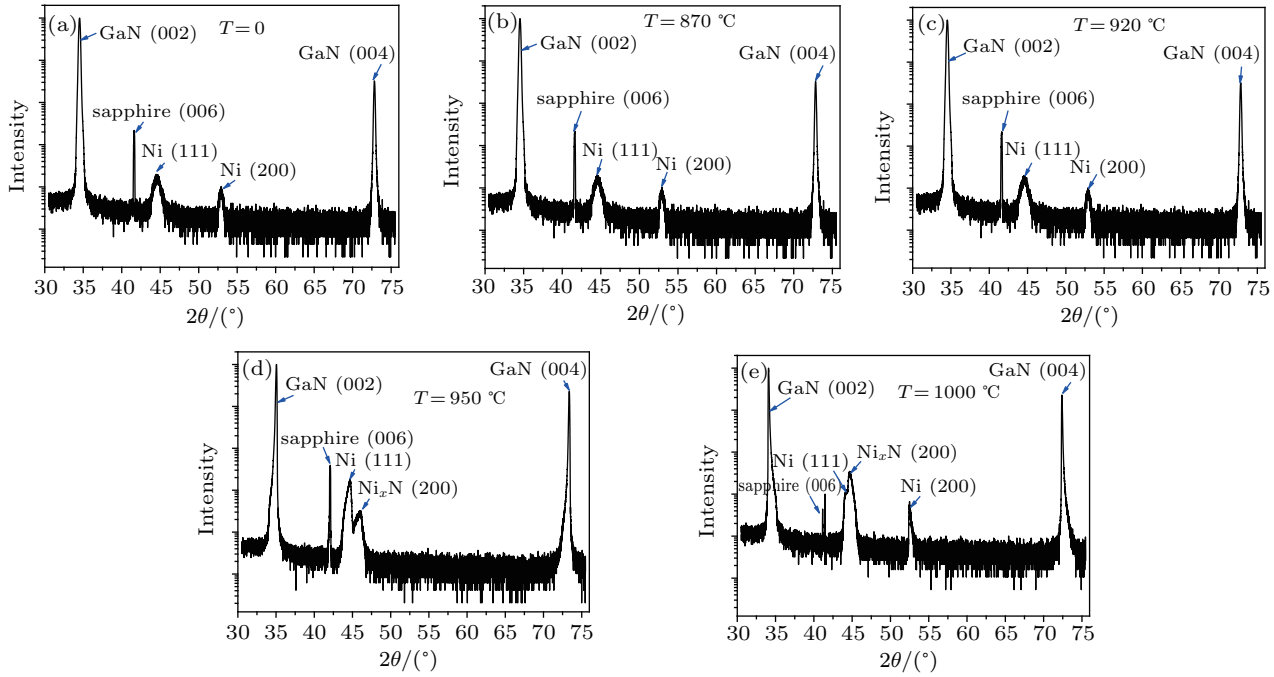


Fig. 6. XRD spectra of Ni film on the GaN (0001) substrate after annealing at different temperatures: (a) as-grown, (b) 870 °C, (c) 920 °C, (d) 950 °C, (e) 1000 °C.

Figure 7 shows the XRD spectra of the annealed Ni films on the sapphire (0001) substrate. The XRD spectra of the as-grown and annealed Ni films not only show the peak at 41.6° from the sapphire (006) but also the Ni (111) peak at 44.5°. For the Ni (111) peak, the full width at half maximum (FWHM) of the as-grown film is 2.753°, and the wide FWHM indicates the polycrystalline nature of the Ni. As the annealing temperature reaches 800 °C, the FWHM of the Ni (111) peak decreases to 0.720° and its intensity strengthens. And the FWHM even reaches 0.476° after annealing at the high

temperature of 900 °C. The trend indicates that the Ni film has a crystallization process in addition to the self-assembly process in high-temperature annealing. The crystallite size of the Ni is evaluated using the Debye–Sherrer equation[13]

$$d_{\mathrm{XRD}} = \frac{0.89\lambda}{(\beta - \beta_0)\cos\theta},$$

where d_{XRD} is the volume average diameter of the crystallite, λ the Cu $K\alpha 1$ wavelength, and β_0 the instrumental line broadening found experimentally from sintered Ni samples (0.148° (2θ) for Ni). The crystallite size is calculated to be 4.23 nm for the as-grown Ni film. The size reaches up to 33.58 nm as the annealing temperature increases up to 900 °C. Table 1 lists the detailed parameters of the Ni self-assembled particles.

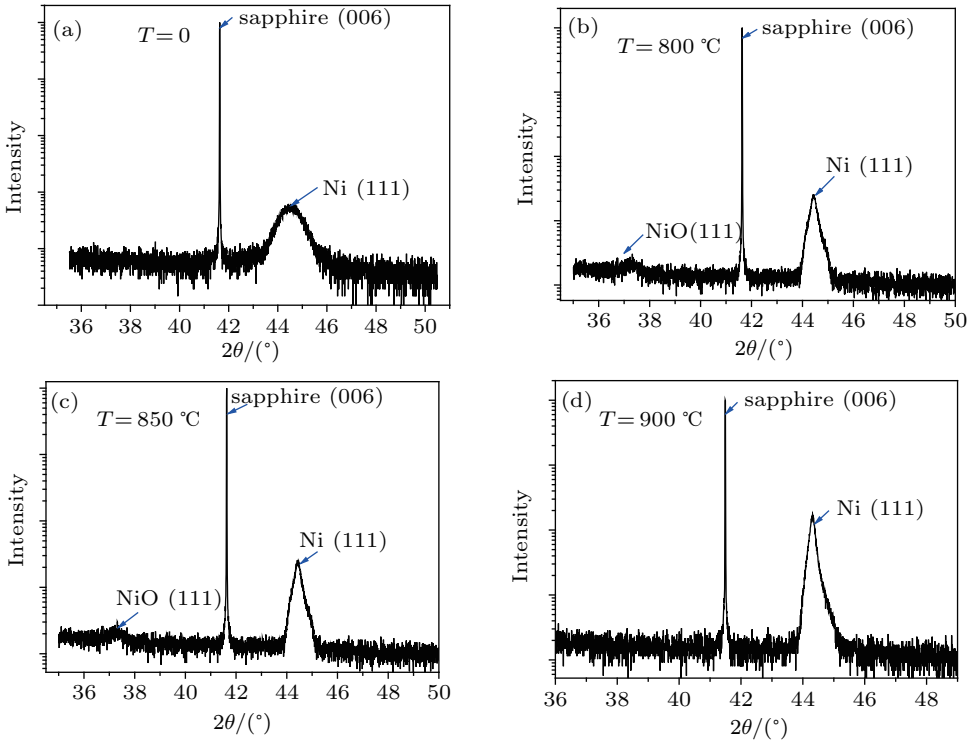


Fig. 7. XRD spectrum of Ni film on the sapphire (0001) substrate after annealing treatment: (a) 0, (b) 800 °C, (c) 850 °C, (d) 900 °C.

Table 1. Parameters of the self-assembled particles on the sapphire (0001) substrate.

Annealing temperature/(°)	Diameter/nm	Number	FWHM/(°)	Crystallite size/nm
800	175	186	0.720	19.26
850	225	101	0.699	19.99
900	250	63	0.476	33.58

In addition, the NiO (111) peak around 37.3° appears for the annealed sample at 800 °C, which confirms the NiO formation. This is due to the Ni diffusion between the sapphire (0001) and Ni particles. As mentioned above, the substrate has a large effect on the self-assembly process. The Si (111) substrate leads to a failure of the self-assembly of Ni particles due to the Si–N layer formation (Fig. 8(c)). The Si–N interlayer naturally forms at the Ni and Si (111) interface at 900 °C in Fig. 8(b). This fact is confirmed by the peak around 33° in the XRD spectrum (this XRD spectrum is not shown in the figure), which is consistent with reports.[12,15,16] The Si–N interlayer as a buffer layer causes self-assembly failure. In contrast, with GaN/sapphire (0001) as the substrates, Ni self-assembly is promoted. Generally, the deposition of the Ni film on the sapphire/GaN (0001) substrates is typically far from equilibrium. The Volmer–Weber growth mode is even observed in the as-deposited process due to the great difference of the surface free energy between the sapphire/GaN (0001) and the Ni.[8] During high temperature annealing, Ni atoms can get enough energy and then diffuse on the surface to agglomerate metal 3D islands. This fact not only affects mass transport but also causes a re-equilibrium process to minimize the system energy. These factors promote the achievement of the self-assembly of Ni particles.

However, there still remain great differences between the sapphire (0001) and the GaN (0001). (i) The Ni film on the sapphire (0001) substrate is assembled into particles at 900 °C compared with that on the GaN (0001) substrate at 1000 °C, and the Ni self-assembly process on the sapphire (0001) substrate loses the stage of the Ni network structure. (ii) The Ni

particle shape is spherical for the sapphire (0001) substrate, and truncated-cone for the GaN (0001) substrate. (iii) A Ni–N interlayer forms between the Ni particles and the GaN (0001) substrate. Actually, all these great differences depend strongly on the interlayer formation. As we know, the heat of formation of the oxide, ΔH, is -241 kJ/mol for Ni with O atoms, whereas that of Al is -1054.9 kJ/mol. Since ΔH for Ni is about one fifth that of Al, the Ni growth on the sapphire (0001) results in little interaction with the substrate. This interaction is so weak that it cannot induce a Ni–O interlayer in the as-grown Ni/sapphire (0001) system.[8,14] But, at the annealing temperature of 800 °C, a NiO layer appears due to the Ni diffusion between the sapphire (0001) and the Ni crystal lattice at high temperature. As the temperature increases up to 900 °C, the NiO has decomposed, and even joins in the self-assembly process (see Fig. 7(d)). However, the Ni/GaN (0001) system has strong enough interaction to form a Ni–N interlayer in the as-grown process. The Ni–N interlayer strongly affects the mass transport of the Ni atoms on the surface, which results in the truncated-cone particles.

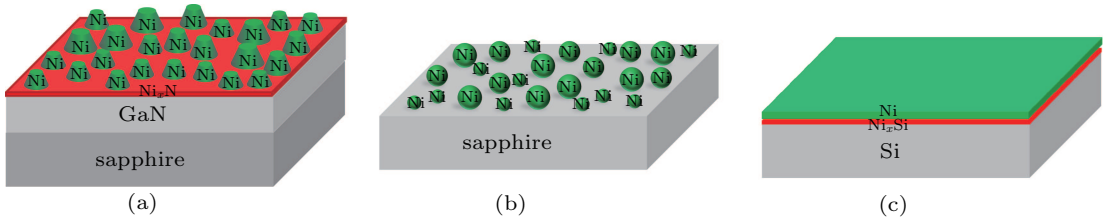


Fig. 8. Model of the Ni self-assembly process on the different substrates: (a) GaN (0001), (b) sapphire (0001), (c) Si (111).

4. Conclusion

We attempt to apply GaN (0001), Si (111) and sapphire (0001) substrates for Ni self-assembly using thermal annealing treatment. The results indicate that GaN/sapphire (0001) substrates are fit for self-assembled Ni particles. For the Si (111) substrate, self-assembly fails due to the formation of a Si–N interlayer. However, for the GaN/sapphire (0001) substrates, there remain great differences in the Ni self-assembly process. (i) The Ni film on the sapphire (0001) substrate is assembled into particles at 900 °C compared with that on the GaN (0001) substrate at 1000 °C, and the Ni self-assembly process on the sapphire (0001) substrate loses the stage of the Ni network structure. (ii) The Ni particle shape is spherical for the sapphire (0001) substrate, and truncated-cone for the GaN (0001) substrate. (iii) A Ni–N interlayer forms between the Ni particles and the GaN (0001) substrate. All these differences are attributed to the interlayer formation between the Ni and the GaN/sapphire (0001) substrates. This interlayer plays a key role in the self-assembly of Ni particles.

References

[1] Chiu C H, Lu T C, Huang H W, Lai C F, Kao C C, Chu J T, Yu C C, Kuo H C, Wang S C, Lin C F and Hsueh T H 2007 *Nanotechnology* **18** 445201
[2] Yang G F, Xie F, Tong Y Y, Chen P, Yu Z G, Yan D W, Xue J J, Zhu H X, Guo Y, Li G H and Gao S M 2015 *Mat. Sci. Semicon. Proc.* **30** 694
[3] Zhao S M and Zhuang P 2014 *Chin. Phys. B* **23** 054203
[4] Henley S J and Carey J D 2005 *Phys. Rev. B* **72** 195408
[5] Facsko S, Dekorsy T, Koerdt C, Trappe C, Kurz H, Vogt A and Hartnagel H L 1999 *Science* **285** 1551
[6] Oh Y J, Ross C A, Jung Y S, Wang Y and Thompson C V 2009 *Small* **5** 860
[7] Tiberto P, Gupta S, Bianco S, Celegato F, Martino P, Chiolerio A, Tagliaferro A and Allia P 2011 *J. Nanopart. Res.* **13** 245
[8] Aggarwal S, Ogale S B, Ganpule C S, Shinde S R, Novikov V A, Monga A P, Burr M R and Ramesh R 2001 *Appl. Phys. Lett.* **78** 1442
[9] Carey J D, Ong L L and Silva S R P 2003 *Nanotechnology* **14** 1223
[10] Chhowalla M, Teo K B K, Ducati C, Rupesinghe N L, Amaratunga G A G, Ferrari A C, Roy D, Robertson J and Milne W I 2001 *J. Appl. Phys.* **90** 5308
[11] Yu C C, Chu C F, Tsai J Y, Huang H W, Hsueh T H, Lin C F and Wang S C 2002 *Jpn. J. Appl. Phys.* **41** L910
[12] Kim S I, Lee S R, Ahn K M and Ahn B T 2010 *J. Electrochem. Soc.* **157** H231
[13] Julies B A, Knoesen D, Pretorius R and Adams D 1999 *Thin Solid Films* **347** 201
[14] Diebold U, Pan J M and Madey T E 1995 *Surf. Sci.* **331–333** 845
[15] Richardson J T, Scates R and Twigg M V 2003 *Appl. Catal. A: Gen.* **246** 137
[16] Detavernier C, Sweet J J and Lavoie C 2008 *J. Appl. Phys.* **103** 113526